fire

MDPI

*Article*

# Mechanism Analysis of Monnex Fire Extinguishing Performance and Particular Burning Fragmentation Phenomenon

**Sai Yao [1], Zilong Liang [1], Zixuan Zhang [1], Suqin Chen [1], Lijing Wang [1], Mingchao Wang [2,*] and Haijun Zhang [1,*]**

[1] School of Safety Science and Engineering, Civil Aviation University of China, Tianjin 300300, China; s_yao@cauc.edu.cn (S.Y.); lzl13820882361@163.com (Z.L.); zzx_130026@163.com (Z.Z.); csq000109@163.com (S.C.); ljwang@cauc.edu.cn (L.W.)

[2] College of Science, Civil Aviation University of China, Tianjin 300300, China

* Correspondence: mingchaowang0@163.com (M.W.); hjzhang_ahu@163.com (H.Z.)

**Abstract**

Monnex has become the most efficient dry powder extinguishing agent due to its unique fire extinguishing mechanism—the "burning fragmentation" phenomenon. To study the fire extinguishing mechanism of Monnex in detail and elucidate the process of its "burning fragmentation" phenomenon, we have examined the microstructure changes and compositions of Monnex powder during its thermal decomposition process. The results indicate that Monnex undergoes complex iterative reactions and produces explosive intermediates ($NH_4NO_3$, KCN, and $KN_3$) when entering the fire. Upon reaching the temperature of 240 °C, the explosive substance is completely pyrolyzed and undergoes a mini- burning fragmentation, resulting in the decomposition of Monnex powder into particles and the release of a large amount of inert gases and free radicals. This is the reason why Monnex has become an optimal dry powder. Toxic substances KCN and KOCN were found during the whole pyrolysis process, so personal protection should be paid attention to in practical applications. Our research not only improves the understanding of the Monnex fire extinguisher, but also provides important scientific evidence for the development of fire extinguishing technologies and environmentally friendly fire protection materials.

**Keywords:** Monnex; extinguishing mechanism; burning fragmentation; explosive components

## 1. Introduction

Fire extinguishing powders have garnered significant attention due to the advantages of high extinguishing efficiency, low cost, and convenient storage, which makes them potential alternatives to halon extinguishers in various fire protection fields [1,2]. Traditional dry powder extinguishing agents, such as BC and ABC dry powder, are widely used for fire protection [3–5]. However, the relatively large particle size of conventional dry powders limits their ability to achieve superior fire extinguishing performance [6,7]. Nowadays, the development trends in this field mostly focus on efficient ultrafine dry powder [8–12]. Their smaller particle sizes, larger specific surface areas, and lighter momentum properties help to achieve excellent fire extinguishing efficiency. However, ultrafinedry powder fire extinguishing agents require 90% of the particles below 20 μm (or even 15 μm), which undoubtedly leads to easy agglomeration and process complexity [13–17]. Therefore, it is imperative to balance the relationship between the particle size and extinguishing effect, and explore more economical and industrialized dry powder fire extinguishing agents.

Monnex dry powder, as an efficient BC dry powder fire extinguishing agent, is an excellent choice in the fields of petrochemical facilities and aviation applications [18–20]. It is a

Check for updates

Academic Editors: Junchao Zhao, Ruiyu Chen and Grant Williamson

Received: 25 March 2026
Revised: 2 June 2026
Accepted: 14 July 2026
Published: 16 July 2026

**Copyright:** © 2026 by the authors. Licensee MDPI, Basel, Switzerland. This article is an open access article distributed under the terms and conditions of the Creative Commons Attribution (CC BY) license.

urethane salt generated by the reaction of $KHCO_3$ or $NaHCO_3$ with urea, and its empirical formula is $MC_2N_2H_3O_3$ (M represents the atom of potassium K or sodium Na) [21–24]. Notably, the critical particle size of Monnex dry powder (50 μm) is significantly larger than that of ABC and other BC powders (20 μm) [19,24], which means that Monnex can exhibit outstanding fire extinguishing efficiency without ultrafine processing, thereby greatly simplifying the production process. It is reported that the fire extinguishing efficiency of Monnex dry powder based on potassium bicarbonate is 5–6 times that of $NaHCO_3$ dry powder, and 2–3 times that of $KHCO_3$ dry powder [25,26].

To delve deeply into the high fire extinguishing efficiency of Monnex, researchers have found its distinctive 'burning fragmentation' phenomenon. Specifically, when exposed to the high temperatures within the combustion zone, Monnex dry powder would explode and/or decrepitate into tiny particles with a larger surface area, enabling it to rapidly quench the free radicals (H· and OH·) in the fire and terminate the chain reaction of the flame propagation, thus achieving rapid control and extinguishing of fires [26]. Despite the confirmed fire extinguishing efficiency of Monnex dry powder, there is currently a lack of research on the details of its extinguishing process and by-product formation, particularly the underlying reasons behind its 'burning fragmentation' phenomenon at elevated temperatures.

In view of the inadequate research on the fire extinguishing mechanism of Monnex, a series of tests (X-ray Diffraction (XRD), scanning electron microscopy (SEM), Brunauer–Emmett–Teller (BET) surface area analysis, and thermogravimetric analysis coupled with Infrared Spectroscopy (TG-IR)) were applied to analyze the fire extinguishing behavior and pyrolysis products of Monnex. By identifying the key intermediates that trigger the fragmentation reaction, this work not only elucidates the fire extinguishing mechanism of Monnex but also provides a plausible explanation for the 'burning fragmentation' phenomenon, enhancing the understanding of Monnex fire extinguishing agent.

## 2. Materials and Methods

### *2.1. Materials and Sample Preparation*

All reagents without further purification were available from chemical reagent companies. Hydrophobic fumed silica and ammonium dihydrogen phosphate were obtained from Shanghai McLin Biochemical Technology Co., Ltd., Shanghai, China. Urea and potassium bicarbonate were purchased from Shandong Xiya Chemical Technology Co., Ltd., Zaozhuang, China. Heptane was purchased from Tianjin Kemiou Chemical Reagent Co., Ltd., Tianjin, China.

*The preparation of Monnex powder.* Firstly, the precursor of Monnex was obtained by mixing potassium bicarbonate (29.1 g) and urea (20.9 g) in a horizontal planetary mill (FOCUCY-F-P4000E) at 250 r/min for 1 h. Subsequently, deionized water of 30% solid mass was added to the precursor and continuously stirred for 15 min to form a milky white colloid. The Milky white colloids are then placed in a hydrothermal reactor at 140 °C for 3 h, followed by cooling to room temperature (RT). The Monnex particles were obtained after the hydrothermal products were placed in a 60 °C oven for 4 h. Finally, the Monnex particles and 5 wt.% hydrophobic silica were refined by horizontal planetary ball mill at a rotational speed of 400 r/min for 40 min with a ball and reagent ratio of 5:1 to obtain Monnex powder.

*The preparation of the comparative sample (ultrafine $NH_4H_2PO_4$ powder).* $NH_4H_2PO_4$ was refined using a horizontal planetary ball mill with a rotational speed of 400 r/min for 40 min. The ratio of balls and reagent was set to 5:1. After drying at room temperature, 5 wt. % hydrophobic silica was incorporated into the dried $NH_4H_2PO_4$, followed by a secondary ball milling treatment to obtain the desired ultrafine $NH_4H_2PO_4$ powder.

### *2.2. Characteristic Method*

The particle size and particle size distribution of the sample powders were measured by the laser particle size analyzer (LS-909, OMEC, Zhuhai, China). The surface morphology was observed by scanning electron microscopy (Regulus 8100, Hitachi, Tokyo, Japan), and the Brunauer–Emmett–Teller and nitrogen adsorption–desorption isotherms were tested by a specific surface and porosity analyzer (ASAP 2460, Micromeritics, Shanghai, China). The curves of thermogravimetric (TG) and differential scanning calorimetry (DSC) were obtained using the synchronous thermal analyzer (STA449F3, Netzsch, Selb, Germany). The X-ray photoelectron spectroscopy (XPS) was collected by Nexsa X-ray, ThermoFisher, Loughborough, UK.

### *2.3. Fire Extinguishing Experiments*

To compare the fire suppression capabilities of ultrafine $NH_4H_2PO_4$ and Monnex powders, a local oil basin test was conducted, aligning with our previous works [7,15]. As illustrated in Figure 1, a small-scale experimental setup included a high-speed camera, a fire extinguishing chamber (1 $m^3$), a data acquisition system, a powder tank, a pressure tank and a nitrogen driving unit. The enclosure was composed of five stainless steel panels and a transparent acrylic plate to observe the flame behavior, with 50 mm diameter holes in the sides and top for natural ventilation. A nozzle with a diameter of 50 mm is located at the center of the top of the fire extinguishing chamber for the release of extinguishing agent. A square oil basin (400 mm × 400 mm × 50 mm) was filled with 200 mL of water and 150 mL of n-heptane as fuel. Four K-type thermocouples (with a diameter of 4 mm) linked to a data acquisition system were used to measure the flame's temperature changes. These thermocouples were positioned 100 mm above the oil basin, with a distance of 100 mm between each thermocouple. The pressure tank incorporated a pressure gauge, inlet pipe, outlet pipe, ball valve, as well as some bolts and nuts. During the fire suppression experiment, the operating pressures were adjusted to 0.1, 0.2, and 0.3 MPa, followed by the release of the sample powder. The initial loading amount of dry powder in the pressure tank before each experiment was 50 g. A high-speed camera was utilized to record the changes in the flame behavior and the time required for fire suppression. To ensure the accuracy and reliability of the fire extinguishing time and powder utilization, each experiment was conducted three times.

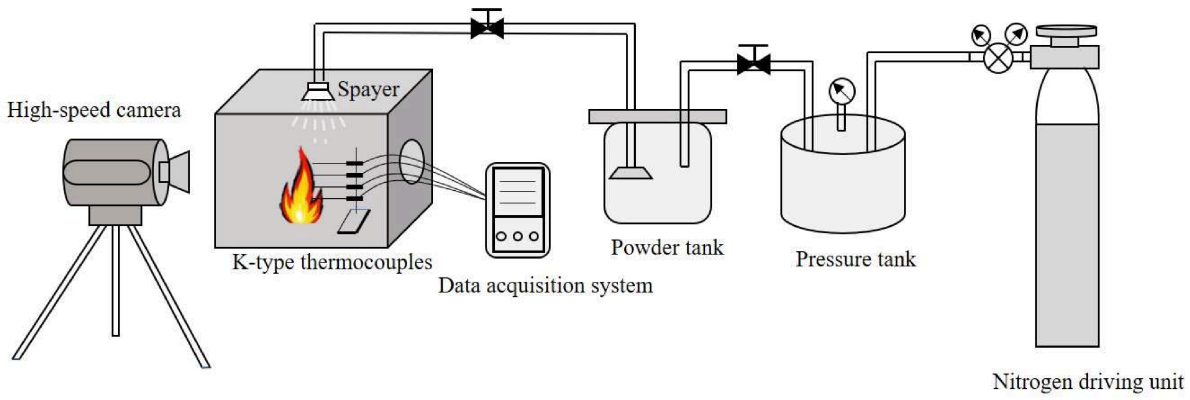



**Figure 1.** The setup of fire extinguishing experiments.

## 3. Results

### *3.1. Material Characterization*

The infrared characteristic peaks of urea, potassium bicarbonate and Monnex were analyzed by FT-IR to determine whether the synthesis process was successful. As shown

in Figure 2, the peaks of urea at 3452 $cm^{-1}$ and 3367 $cm^{-1}$ correspond to the stretching vibration of $NH_2$ group; the peak at 1683 $cm^{-1}$ is attributed to the stretching vibration of C=O group; the peak at 1603 $cm^{-1}$ is the variation in the $NH_2$ group; and the peak at 1468 $cm^{-1}$ could be regarded as bending vibration of C-N group [27]. For $KHCO_3$, the peaks at 3417 $cm^{-1}$, 1403 $cm^{-1}$ and 1008 $cm^{-1}$ correspond to the stretching vibrations of the OH group, and the peak at 1651 $cm^{-1}$ corresponds to the C=O group. Compared with urea and $KHCO_3$, the peaks of Monnex at 3358 $cm^{-1}$, 3213 $cm^{-1}$ and 1670 $cm^{-1}$ belong to the peaks of O-H, N-H and C=O groups, respectively. Specifically, allophanate serves as a component group within Monnex, and its characteristic peak is located at 1726 $cm^{-1}$, which is consistent with previous reports [28]. The IR results demonstrate that urea and $KHCO_3$ generated allophanate under hydrothermal reaction, confirming the successful synthesis of Monnex particles.

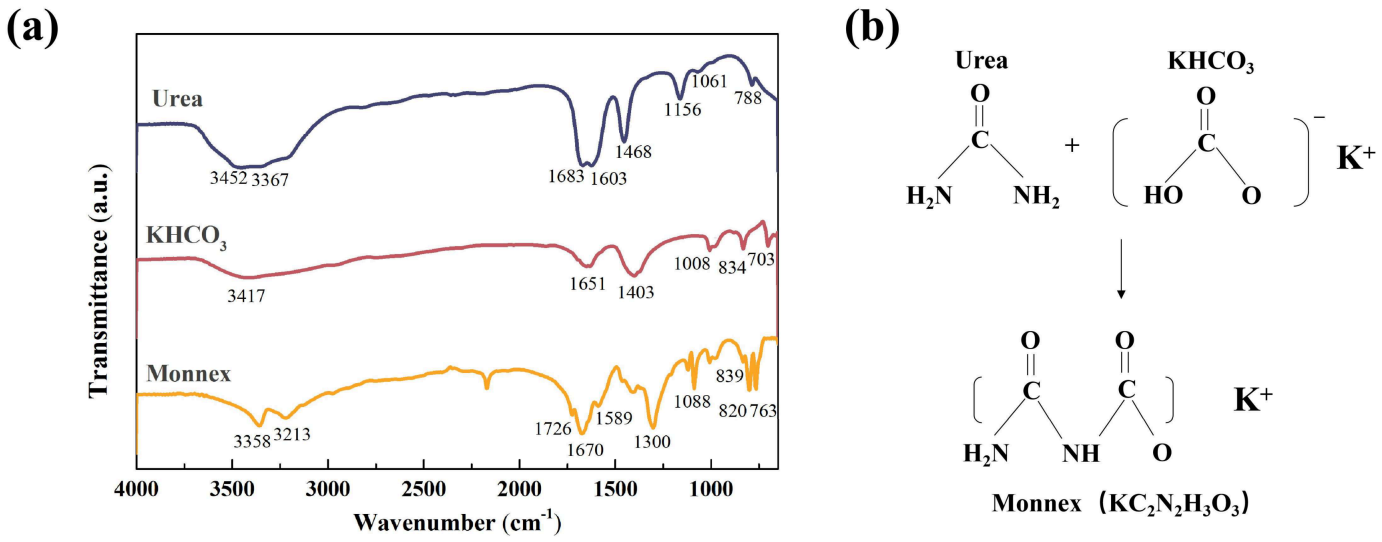



**Figure 2.** (**a**) Infrared diffraction peaks of urea, $KHCO_3$ and Monnex; (**b**) the combination rules of the Monnex.

### *3.2. Particle Distribution and Micromorphology Characterization*

The particle size distribution and micromorphology characterization of powders are primary factors that determine the fire extinguishing performance. During the extinguishing process, particles with sizes smaller than the critical particle size have been proven to exhibit high fire extinguishing capabilities [29,30]. Figure 3a,b present the particle sizes and size distributions of ultrafine $NH_4H_2PO_4$ powder and Monnex powder, respectively. It can be found that 90% of the particles in ultrafine $NH_4H_2PO_4$ powder measure less than 19.829 μm (D90 = 19.829 μm < 20 μm), and 90% of the particles in Monnex powder are smaller than 50.267 μm (D90 = 50.26 μm near 50 μm), which suggests that both powders meet the critical particle size requirements and could achieve optimal fire extinguishing performance.

The microstructures of ultrafine $NH_4H_2PO_4$ powder and Monnex powder also exhibit different morphologies. As shown in Figure 4a,b, the particles of the ultrafine $NH_4H_2PO_4$ powder are densely distributed at the scale of 50 μm. When further magnified to a 5 μm scale, the ultrafine particles show apparent aggregation and form irregular block-like structures driven by the interaction of the coulomb force, high surface free energy and chemical bonds between particles. Compared to the ultrafine $NH_4H_2PO_4$ powder, the microscopic images of Monnex powder (Figure 4c,d) indicate that the particles of Monnex powder are larger, as well as the gap between particles. When enlarged to the scale of 5 μm, the Monnex particles exhibit a relatively loose arrangement, indicating a low tendency for

particle agglomeration in practical production. Simultaneously, the adsorption–desorption curves and characterizations of pore size distribution were shown in Figure 4e,f, with the relevant data summarized in Table 1. The results indicate that the specific surface area (11.24 $m^2/g$) and pore volume (0.03 $cm^3/g$) of the ultrafine $NH_4H_2PO_4$ powder are significantly larger than those of Monnex (2.68 $m^2/g$ and 0.01 $cm^3/g$), which is in accordance with the initially measured particle sizes and microscopic structures.

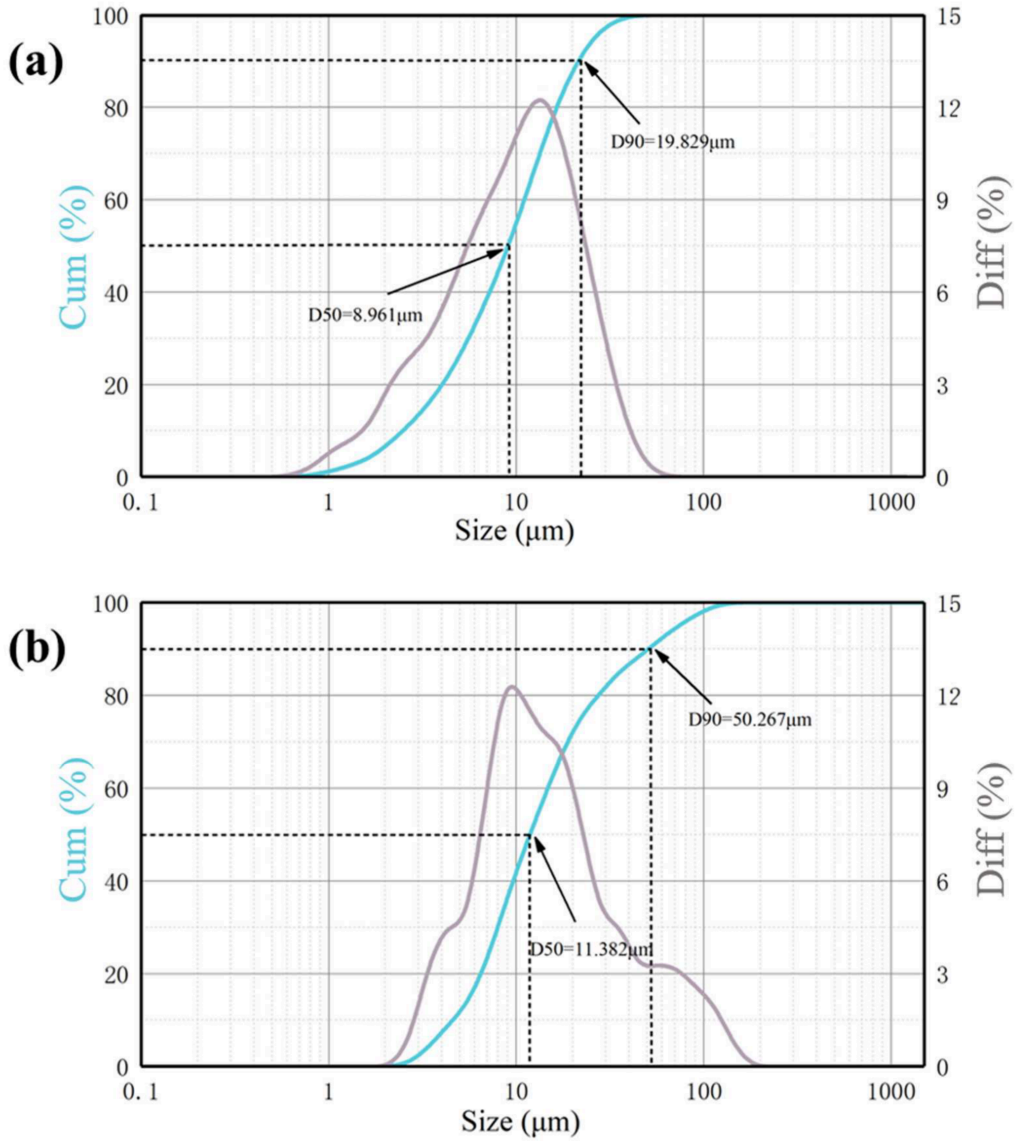



**Figure 3.** The particle size and size distribution of (**a**) ultrafine $NH_4H_2PO_4$ powder; (**b**) Monnex powder. Cum (%) and Diff (%) denote the cumulative percentage and differential percentage, respectively.

**Table 1.** Particle size and BET surface area analysis of two samples.

| Sample | D50 (μm) | D90 (μm) | $S_{BET}$ ($m^2/g$) | $V_{total}$ ($cm^3/g$) |
|---|---|---|---|---|
| ultrafine $NH_4H_2PO_4$ powder | 8.961 | 19.829 | 11.240 | 0.030 |
| Monnex powder | 11.382 | 50.267 | 2.720 | 0.010 |

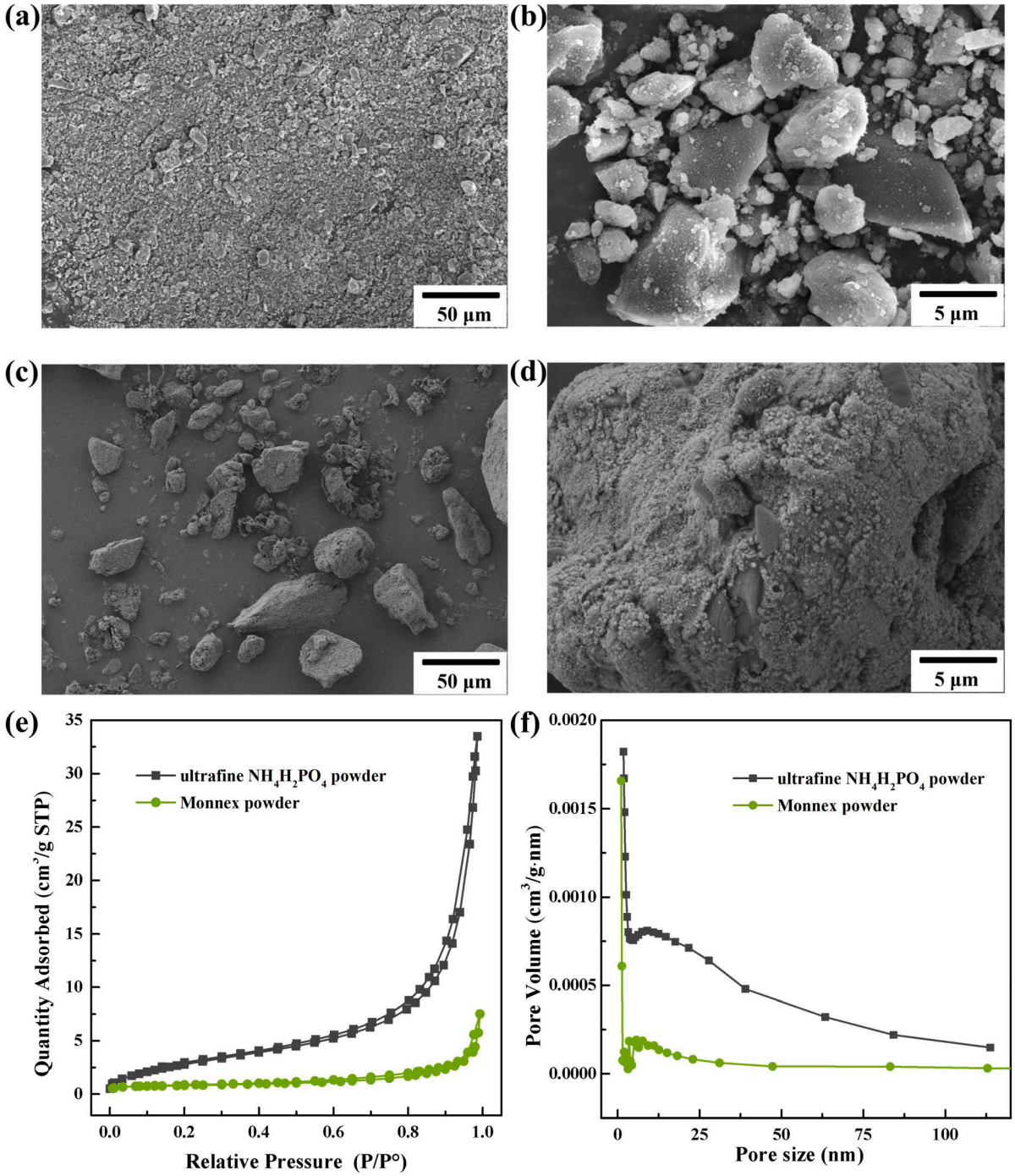



**Figure 4.** Scanning electron microscopy images of (**a**,**b**) ultrafine $NH_4H_2PO_4$ powder and (**c**,**d**) Monnex powder; (**e**) adsorption–desorption curves and (**f**) pore size distribution of ultrafine $NH_4H_2PO_4$ and Monnex powders.

### *3.3. Fire Extinguishing Performance*

A series of fire extinguishing tests under 0.1, 0.2, and 0.3 MPa were conducted to evaluate the fire extinguishing performance of ultrafine $NH_4H_2PO_4$ powder and Monnex powder. Initially, nitrogen gas ($N_2$) without any powder was sprayed into a burning oil basin, and the flame was extinguished after 140 s. Consequently, to eliminate the primary influence of pressurized $N_2$ on fire suppression, a maximum extinguishing time limit of 25 s was set for the subsequent experiments. Before releasing the fire extinguishing agent, the samples were pre-burned for 30 s to stabilize the temperature (about 700 °C). Table 2 lists the applied pressure, extinguishing time, and consumed extinguishant mass

of both powders. The results indicate that the fire extinguishing time and extinguishing agent mass of Monnex are both less than those of ultrafine $NH_4H_2PO_4$ dry powder at the same pressure, demonstrating superior fire extinguishing performance. Moreover, the fire suppression advantage of Monnex becomes more pronounced as the pressure increases. Especially, at an applied pressure of 0.2 MPa, the average extinguishing time (5 s) and extinguishing agent mass (6.753 g) of Monnex are almost half that of ultrafine $NH_4H_2PO_4$ (13 s, 13.623 g). These two sample screenshots of fire extinguishing experiments at 0.2 MPa were also shown in Figure 5a,b (videos in Supporting Files).

**Table 2.** Fire extinguishing time and agent mass consumed of ultrafine $NH_4H_2PO_4$ and Monnex powder under varying pressures.

| Sample Power | Pressure (MPa) | Average [Fire Extinguishing Time] (s) | Average [Agent Mass Consumed] (g) |
|---|---|---|---|
| ultrafine $NH_4H_2PO_4$ powder | 0.1 | 25 [25, 23, 26] | 20.5 [20.6, 20.5, 20.5] |
| | 0.2 | 13 [13, 14, 13] | 13.6 [13.7, 13.8, 13.4] |
| | 0.3 | 9 [9, 9, 10] | 7.0 [6.9, 7.1, 7.1] |
| Monnex powder | 0.1 | 18 [18, 18, 19] | 18.3 [18.4, 18.1, 18.4] |
| | 0.2 | 5 [5, 4, 5] | 6.8 [6.8, 6.5, 7.0] |
| | 0.3 | 2 [2, 2, 3] | 5.3 [5.3, 5.2, 5.5] |

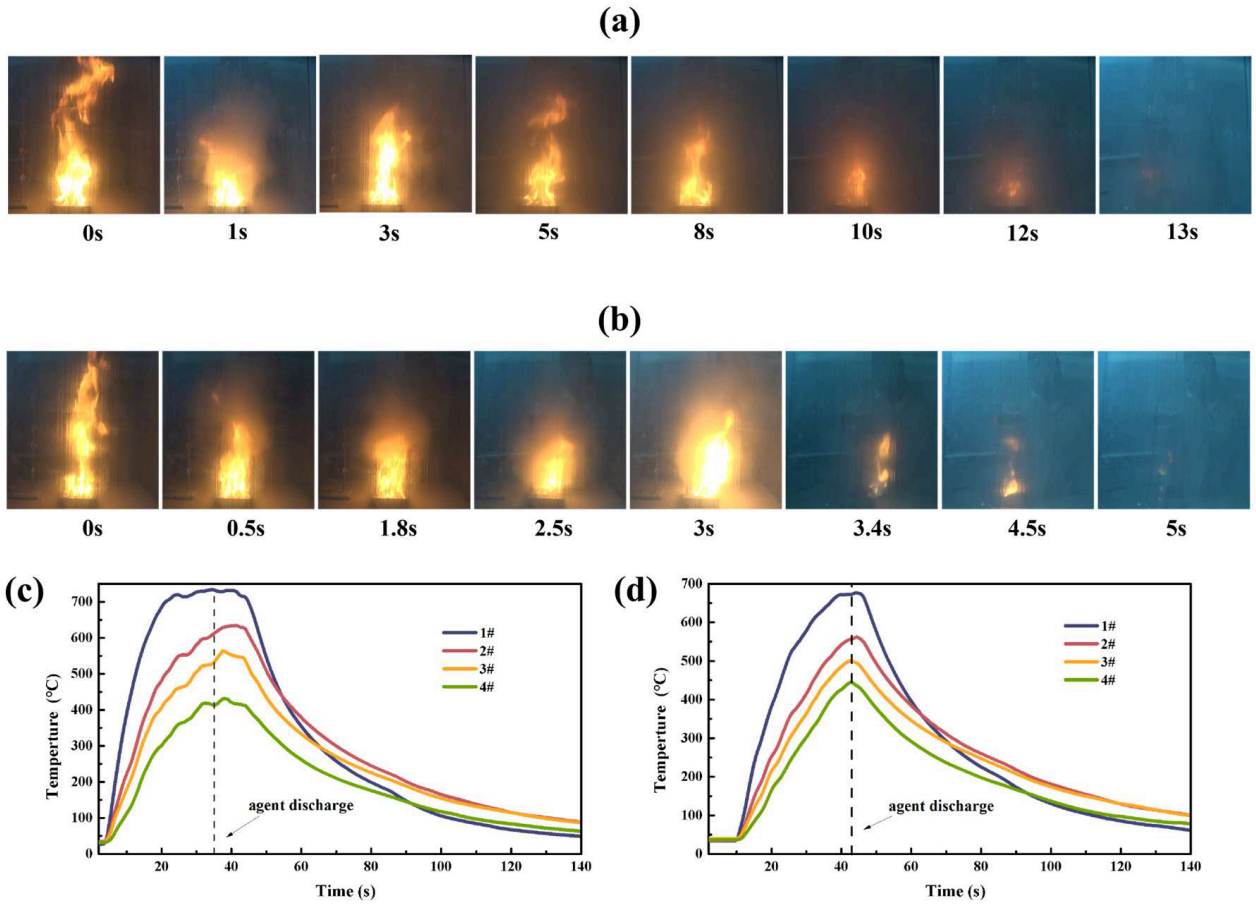



**Figure 5.** Images of the fire extinguishing test procedures of (**a**) ultrafine $NH_4H_2PO_4$ powder and (**b**) Monnex powder at 0.2 MPa; temperature variation curves of (**c**) ultrafine $NH_4H_2PO_4$ powder and (**d**) Monnex powder.

To compare the impact of fire extinguishing agents on the temperature of fire scenes, the temperature changes were also tested (Figure 5c,d). When two types of powders enter the fire, the temperature curves begin to fluctuate, followed by a downward trend. It is worth noting that due to the difference in fire extinguishing performance between the two samples, their temperature curves also exhibit different patterns. When ultrafine $NH_4H_2PO_4$ powder enters the fire scene, the fire temperature undergoes a relatively long period of temperature fluctuations before rapidly decreasing. In contrast, the fire temperature of Monnex drops rapidly with almost no fluctuations, further confirming that Monnex has a shorter extinguishing time and superior cooling effect. Additionally, due to its large initial particle size, Monnex could effectively avoid the interference of the fire plume and reach the base of the flame, which means Monnex can accurately target the fire source and is more suitable for local fire suppression devices.

## 4. Discussion

Given the unique and efficient fire extinguishing ability of Monnex powder, it is necessary to further study its fire extinguishing mechanism. Due to the complexity of actual fire scene reactions, the thermal decomposition process of fire extinguishing was explored to figure out the fire extinguishing mechanism [31–33]. Firstly, the thermogravimetric analysis (TGA) and differential thermogravimetric analysis (DTG) curves (Figure 6a,b) of the two fire extinguishing agents are used to show the differences in thermal performance. According to the thermogravimetric curves, it is found that the thermal decomposition process of ultrafine $NH_4H_2PO_4$ can be divided into two stages: the first stage reaches the peak of thermal decomposition at about 200 °C, and the second stage reaches the maximum rate of thermal decomposition at 600 °C. In contrast, the pyrolysis behavior of Monnex occurs earlier, with pyrolysis starting at 100 °C and reaching its maximum thermal decomposition rate between 100 °C and 200 °C. Additionally, a minor thermal decomposition peak of Monnex is observed at approximately 780 °C. The pyrolysis process of Monnex powder is mainly concentrated between 100 °C and 200 °C, indicating that it mostly decomposes in this temperature range. Furthermore, according to the differential scanning calorimetry (DSC) curve analysis of the two sample powders (Figure 6c), the heat absorption of Monnex is significantly lower than that of $NH_4H_2PO_4$. Therefore, it can be inferred that the fire extinguishing advantage of Monnex is not endothermic cooling, but rapid quenching of free radicals and interruption of reaction chains, thus achieving rapid fire extinguishing.

The morphological changes in Monnex within the fire were also studied. To simulate the real fire environment, Monnex was calcined at room temperature, 190 °C and 240 °C, respectively. As shown in Figure 7, Monnex particles remain intact with smooth surfaces at room temperature. After calcination at 190 °C, the particle surface becomes rough and forms a honeycomb-like structure, indicating the generation of large amounts of gas at high temperatures, which is consistent with the rapid weight loss observed in thermogravimetric analysis. When the calcination temperature exceeds 240 °C, the giant skeleton particles decompose into small particles, and their specific surface area increases rapidly from 2.68 $m^2/g$ at room temperature to 3.78 $m^2/g$ (Table 3), which confirms that Monnex experienced similar small-scale fragmentation before 240 °C.

**Table 3.** BET surface area analysis at different temperatures.

| Sample | $S_{BET}$ ($m^2/g$) | $V_{total}$ ($cm^3/g$) | D (nm) |
|---|---|---|---|
| Monnex (RT) | 2.68 | 0.007 | 17.03 |
| Monnex (190 °C) | 2.72 | 0.010 | 20.96 |
| Monnex (240 °C) | 3.78 | 0.016 | 21.10 |

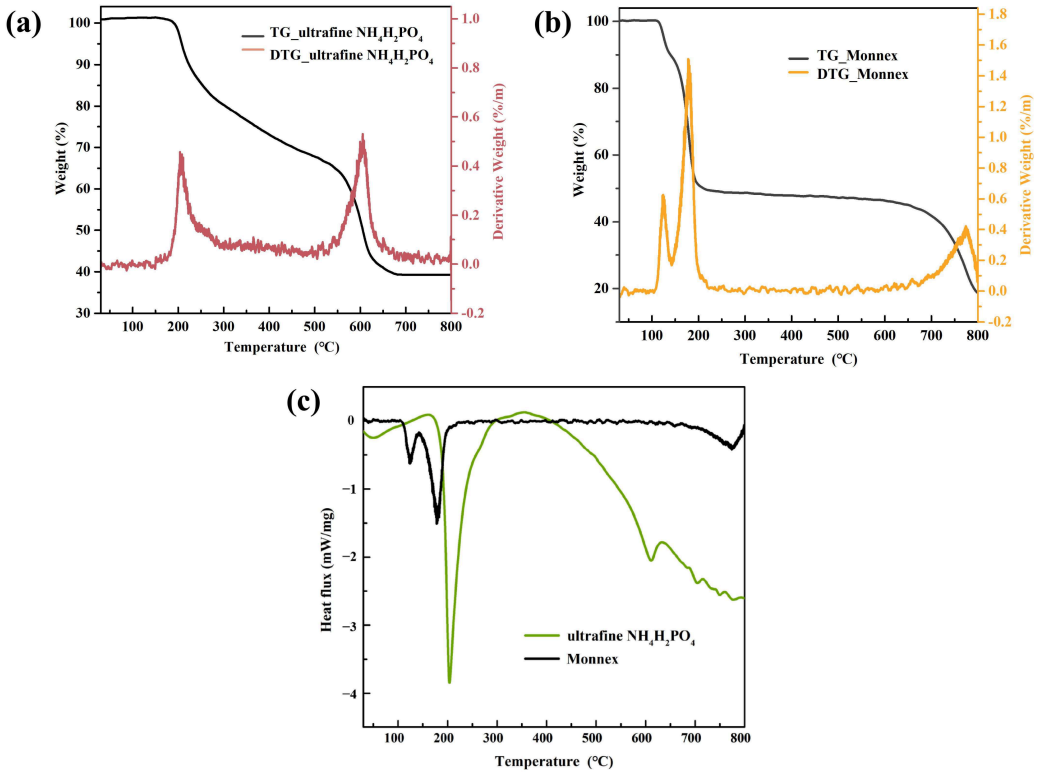



**Figure 6.** Thermogravimetric and derivative thermogravimetric curves of (**a**) ultrafine $NH_4H_2PO_4$ powder and (**b**) Monnex powder; (**c**) differential scanning calorimetry curves of ultrafine $NH_4H_2PO_4$ and Monnex powders.

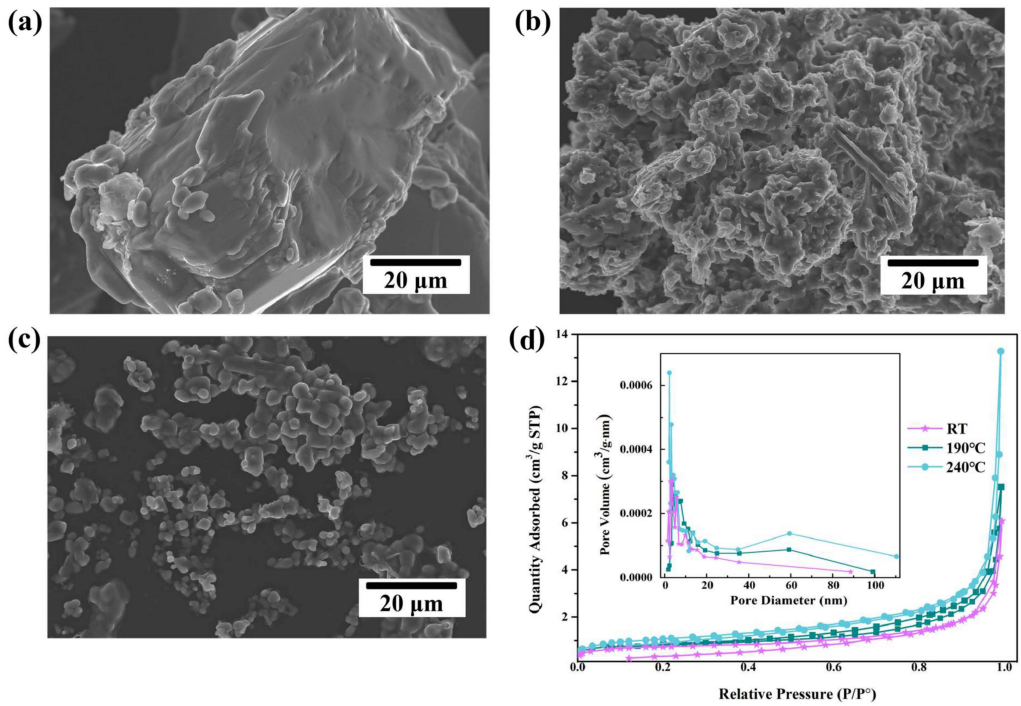



**Figure 7.** (**a**–**c**) SEM changes in Monnex grain calcined at RT, 190 °C, and 240 °C; (**d**) adsorption and desorption and pore size distribution curves of Monnex grain calcined at RT, 190, and 240 °C.

To further elucidate the fragmentation phenomenon and figure out the decomposition products of Monnex, TG-IR and XRD were used to detect the products of the Monnex in the thermal decomposition process. Based on its three-dimensional plot (Figure 8a), it

can be found that the gaseous products are concentrated between 100 and 300 °C, which is approximately consistent with the temperature range at which Monnex undergoes fragmentation. The specific gaseous products of Monnex at temperatures of 120 °C, 190 °C, 240 °C, and 700 °C were analyzed in Figure 8b. The results indicate that the pyrolysis of Monnex mainly produces small gaseous molecules such as $CO_2$, $H_2O$ and $NH_3$ at 120 °C. As the temperature gradually increases, there is a noticeable trend of increasing content in the released $CO_2$, $H_2O$ and $NH_3$, and low-molecular-weight compounds containing C=N, N=O, and N-O groups, some of which were subsequently confirmed to be potentially $HNO_3$ or $N_2O$ gases (see Figure 9b). When the temperature reaches above 700 °C, the residual substances in the gas phase are almost exclusively $CO_2$.

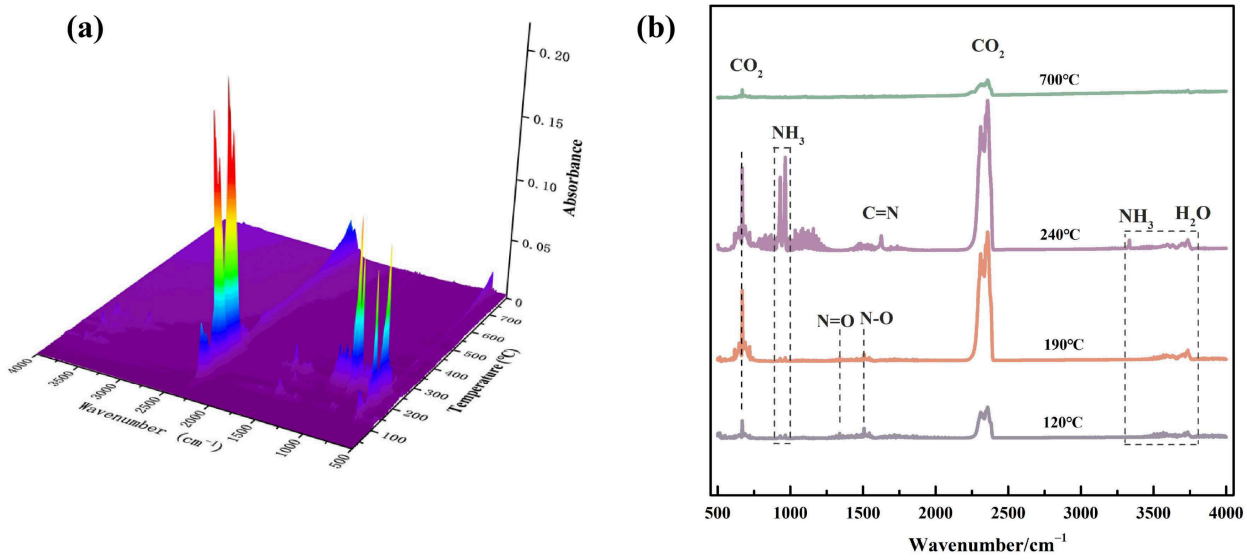



**Figure 8.** (**a**) Three-dimensional TG-IR spectra; (**b**) absorption spectra of pyrolysis products at different temperatures of Monnex powder.

Moreover, the results of the XRD test were shown in Figure 9. Because Monnex is originally prepared by the reaction of $KHCO_3$ and urea, there may be some unreacted raw materials remaining (seen in the peaks a and b at room temperature in Figure 9a). When the temperature attains 120 °C, novel peaks corresponding to $NH_4NO_3$, KCN, and $KNH_2$ emerge in the spectroscopic analysis. As the temperature escalates, the calcined products evolve: the generation of $KNO_3$ at 190 °C, followed by $KN_3$ and $KNO_2$ at 240 °C. Ultimately, the resultant products stabilize into KOH and stable KOCN. Based on these observations, we infer that the chemical reactions occurring during the fragmentation of Monnex are depicted in Figure 9b. $NH_4NO_3$, KCN, and $KN_3$ are thermally sensitive and explosive substances that are prone to small-scale explosions at high temperatures, which provides a reasonable explanation for the generation of combustion fragments of Monnex. Specifically, as the temperature gradually rises from room temperature to 120 °C, $NH_4NO_3$ begins to decompose, yielding $HNO_3$ and $NH_3$. As the temperature further increases, the decomposition rate of $NH_4NO_3$ accelerates significantly, and it rapidly decomposes into $N_2O$ and $H_2O$. When the temperature climbs to 240 °C, the decomposition of $NH_4NO_3$ becomes more intense, accompanied by the occurrence of fragmentation. The fire suppression pathway is illustrated in Figure 9c. Various by-products (e.g., $NH_4NO_3$, $KNH_2$, KOH, $NH_3$, $N_2O$) play a significant role in the fire suppression process. These burning fragmentation products of Monnex can react with H· and OH· radicals in the fire environment, effectively terminating the chemical chain reactions and achieving flame suppression. Concurrently, the fragmentation process releases a substantial amount of

water vapor and inert gases. These gases not only help to lower the temperature but also significantly dilute the oxygen concentration in the surrounding environment, exerting a potent inhibitory effect on flame combustion.

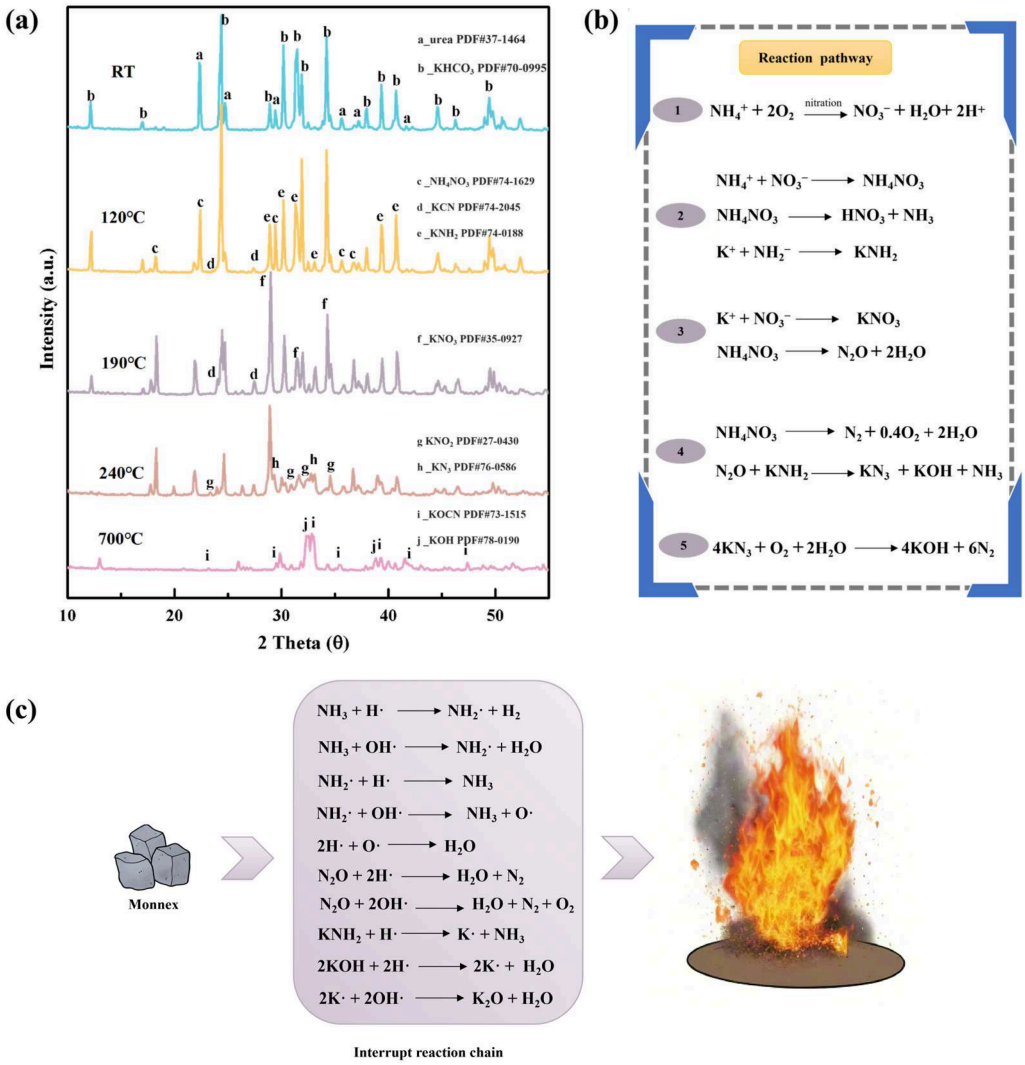



**Figure 9.** (**a**) XRD analysis of components at different temperatures; (**b**) reaction pathway and (**c**) interrupted reaction chain of Monnex powder.

## 5. Conclusions

In this study, Monnex powder was prepared using $KHCO_3$ and urea as raw materials. The morphological changes in the samples after entering the fire were studied by microscopic characterization. TG-DSC, TG-IR, and XRD were used to analyze the compositional changes in Monnex after entering the fire. The following conclusions can be drawn:

(1) Monnex powder exhibits superior fire suppression effectiveness compared to ultrafine $NH_4H_2PO_4$ powder in extinguishing oil fires. Due to its relatively larger particle size, it is more suited for localized fire suppression devices (directional spray systems).

(2) It was found by TG-DSC that the heat absorption and decomposition rate of Monnex powder were lower than those of ultrafine $NH_4H_2PO_4$ powder, but the fire extinguishing effect of Monnex was better than that of ultrafine $NH_4H_2PO_4$ powder. This shows that the primary fire extinguishing mechanism of Monnex is not to reduce the fire temperature by heat absorption. Instead, the large particles entering the fire break into small particles and then quickly release a large amount of gas and free radicals to achieve the purpose of extinguishing the fire.

(3) XRD and TG-IR analysis indicate that the combustion products of Monnex, namely $NH_4NO_3$, KCN, and $KN_3$, may be the causes of the bursting phenomenon. Additionally, the extensive production of water vapor and inert gases significantly dilutes the oxygen concentration in the surrounding environment, exerting an inhibitory effect on flame combustion.

(4) During the Monnex fire extinguishing process, we detected trace amounts of highly toxic KCN, and its final thermal decomposition products also contained toxic KOCN. Therefore, appropriate protective measures need to be taken when using it.

**Supplementary Materials:** The following supporting information can be downloaded at: https://www.mdpi.com/article/10.3390/fire9070304/s1, Video S1: extinguishment of the burning oil when purging with nitrogen gas without any powder; Video S2: extinguishment process of the ultrafine $NH_4H_2PO_4$ powder at 0.2 MPa; Video S3: extinguishment process of Monnex powder at 0.2 MPa.

**Author Contributions:** Conceptualization, S.Y., M.W. and H.Z.; methodology, S.Y. and Z.L.; validation, Z.Z., S.C. and L.W.; formal analysis, Z.L.; investigation, S.Y., Z.L., Z.Z., S.C. and L.W.; resources, S.Y.; data curation, Z.Z. and L.W.; writing—original draft preparation, Z.L.; writing—review and editing, S.Y.; visualization, S.Y. and Z.L.; supervision, M.W. and H.Z.; funding acquisition, S.Y. and H.Z. All authors have read and agreed to the published version of the manuscript.

**Funding:** Please add: This research was funded by the Fundamental Research Funds for the Central Universities (3122023QD02), Tianjin Science Fund for Distinguished Young Scholars (21JCJQJC00040) and National Natural Science Foundation of China (22306196).

**Institutional Review Board Statement:** Not applicable.

**Informed Consent Statement:** Not applicable.

**Data Availability Statement:** Data will be made available on request.

**Conflicts of Interest:** The authors declare no conflicts of interest.

## References

1. Liu, H.; Zong, R.; Gao, J.; Lo, S.; Niu, S.; Hu, Y. A Good Dry Powder to Suppress High Building Fires. *APCBEE Procedia* **2014**, *9*, 291–295. [CrossRef]
2. Zhao, G.; Xu, G.; Jin, S.; Zhang, Q.; Liu, Z. Fire-Extinguishing Efficiency of Superfine Powders Under Different Injection Pressures. *Int. J. Chem. Eng.* **2019**, *2019*, 2474370. [CrossRef]
3. Li, H.; Hua, M.; Pan, X.; Li, S.; Guo, X.; Zhang, H.; Jiang, J. The Reaction Pathway Analysis of Phosphoric Acid with the Active Radicals: A New Insight of the Fire-Extinguishing Mechanism of ABC Dry Powder. *J. Mol. Model.* **2019**, *25*, 366. [CrossRef]
4. Luo, Z.; Su, Y.; Chen, X.; Zheng, L. Effect of BC Powder on Hydrogen/Methane/Air Premixed Gas Deflagration. *Fuel* **2019**, *257*, 116095. [CrossRef]
5. Zhao, J.; Fu, Y.; Lu, S.; Lu, G.; Xue, F.; Zhang, H. An Improved Method to Determine the Minimum Extinguishing Concentrations of Ultrafine Dry Powder Agents: Taking $NaHCO_3$ and $KHCO_3$ as Examples. *Process Saf. Environ. Prot.* **2023**, *172*, 846–856. [CrossRef]
6. Liang, Z.; Zhou, Z.; Sun, Y.; Huang, Y.; Guo, X.; Cai, G.; Wang, M.; Zhang, H. Fire Extinguishing Performance of Chemically Bonded Struvite Ceramic Powder with High Heat-Absorbing and Flame Retardant Properties. *Materials* **2022**, *15*, 8021. [CrossRef] [PubMed]
7. Jiang, H.; Bi, M.; Li, B.; Zhang, D.; Gao, W. Inhibition Evaluation of ABC Powder in Aluminum Dust Explosion. *J. Hazard. Mater.* **2019**, *361*, 273–282. [CrossRef] [PubMed]
8. Wang, D.; Fan, Z.M.; Deng, L.R.; Wang, X.G. Review on Classification and Application Prospect of Ultrafine Powder Material. *Mater. Sci. Forum* **2015**, *809*, 272–277.
9. Zhou, Y.; Zhao, J.; Fu, Y.; Yu, Z.; Lu, S.; Zhang, H.; Jiang, Y. Study on the Hydrophobic Nano Silica Particles as Flow-Enhancing Additives for Ultrafine Dry Powder Fire Extinguishing Agent. *Adv. Powder Technol.* **2024**, *35*, 104397. [CrossRef]
10. Zhou, Y.; Zhao, J.; Wang, T.; Yu, Z.; Fu, Y.; Jiang, Y.; Cheng, X.; Zhang, H. Design of a high-efficiency ultrafine dry powder fire extinguishing agent incorporated with Fe/ZSM-5 zeolite. *Powder Technol.* **2025**, *462*, 121133. [CrossRef]
11. Liu, Y.; Chen, R.; Wang, Z.; Zhang, R.; Jing, H.; Yu, D.; Pan, R. Effects of thermal aging on the performance of ordinary and novel superhydrophobic and oleophobic ultra-fine dry powder extinguishing agent. *Sci. Rep.* **2025**, *15*, 3668. [CrossRef] [PubMed]
12. Guo, X.; Chen, Y.; Xue, S.; Wang, Z.; Li, J.; Pan, X.; Hua, M.; Jiang, J. Experimental research on the suppression of hydrogen deflagration by flame-retardant composite ultrafine dry powder fire extinguishing agents containing aluminum hydroxide. *Process Saf. Environ. Prot.* **2025**, *198*, 107121. [CrossRef]

13. Lu, G.; Zhao, J.; Zhou, Y.; Fu, Y.; Lu, S.; Zhang, H. Study on Flowability Enhancement and Performance Testing of Ultrafine Dry Powder Fire Extinguishing Agents Based on Application Requirements. *Fire* **2024**, *7*, 146. [CrossRef]
14. Wang, Z.; Zhang, Y.; Liu, Y.; Wang, J.; Zhou, X.; Pan, R. Study on the Pyrolysis and Fire Extinguishing Performance of High-Temperature-Resistant Ultrafine Dry Powder Fire Extinguishing Agents for Aviation Applications. *Molecules* **2024**, *29*, 3500. [CrossRef] [PubMed]
15. Wang, X. Study on Modification Technology of Superfine Dry Powder Fire Extinguishing Agent. *J. Phys. Conf. Ser.* **2023**, *2539*, 012091. [CrossRef]
16. Wang, M.; Zhou, Z.; Liang, Z.; Du, S.; Cai, G.; Wang, X.; Zhou, Y.; Zhang, H. The Preparation and Fire Extinguishing Mechanism Research of a Novel High-Efficiency $KHCO_3$@HM Dry Powder. *Mater. Today Commun.* **2024**, *38*, 107817. [CrossRef]
17. *GB 46996-2025*; Super Fine Powder Fire Extinguishing Agent. State Administration for Market Regulation: Beijing, China, 2025.
18. Ewing, C.T.; Faith, F.R.; Hughes, J.T.; Carhart, H.W. Flame Extinguishment Properties of Dry Chemicals: Extinction Concentrations for Small Diffusion Pan Fires. *Fire Technol.* **1989**, *25*, 134–149. [CrossRef]
19. Fischer, G.; Leonard, J. *The Effectiveness of Fire Extinguishing Powders Based on Small Scale Fire Suppressant Tests*; Naval Research Laboratory: Washington, DC, USA, 1995.
20. Roosendans, D.; Hoorelbeke, P. Industrial System for Mitigation of Vapor Cloud Explosions. *J. Loss Prev. Process Ind.* **2020**, *68*, 104273. [CrossRef]
21. Cottrell, A.G.; Bradford, N.D.; Lovett, T.O. Solid Fire-Extinguishing Compositions. U.S. Patent 3,776,843, 4 December 1973.
22. Hollows, F.B. Preparation of Fire-Extinguishing Material Comprising Heating Biuret with Sodium or Potassium Hydroxide. U.S. Patent 3,642,621, 15 February 1972.
23. Warnock, W.R.; Flatt, D.V.; Eastman, J.R. Fire Extinguishing Composition and Method. U.S. Patent 3,553,066, 5 January 1971.
24. Yan, Y.; Han, Z.; Zhao, L.; Du, Z.; Cong, X. Study on the Relationship Between the Particle Size Distribution and the Effectiveness of the K-Powder Fire Extinguishing Agent. *Fire Mater.* **2018**, *42*, 336–344. [CrossRef]
25. Bennett, J.M.; Bennettech, L. "Black Widow" Thermal Absorptivity-Enhanced Dry Chemical Powder—Recent Evaluations in Various Fire Protection Applications. In *Proceedings of the Halon Options Technical Working Conference*; National Institute of Standards and Technology: Gaithersburg, MD, USA, 2005; pp. 1–14.
26. Guo, Y.; Chang, Z.; Tan, Z. Study on Fire Extinguishing Mechanism of Allophanate Based on Monnex Dry Powder. *Comput. Theor. Chem.* **2023**, *1230*, 114361. [CrossRef]
27. Schaber, P.M.; Colson, J.; Higgins, S.; Thielen, D.; Anspach, B.; Brauer, J. Thermal Decomposition (Pyrolysis) of Urea in an Open Reaction Vessel. *Thermochim. Acta* **2004**, *424*, 131–142. [CrossRef]
28. Qin, R.; Wang, G.; Yang, B. Study on the Method of Lowering the Free-TDI in Prepolymer by Synthesizing Allophanate. *Xiandai Tuliao Yu Tuzhuang* **2006**, *11*, 15.
29. Liu, A.; Lu, X.; Zhou, X.; Xu, C.; Liang, X.; Xiong, K. Experimental Investigation on Suppression of Methane Explosion Using $KHCO_3$/Zeolite Composite Powder. *Powder Technol.* **2023**, *415*, 118157. [CrossRef]
30. Zhao, J.; Xue, F.; Fu, Y.; Lu, S.; Zhang, H. Insights into the Particle Diameter and Base Chosen for Dry Powder Fire Extinguishing Agents. *Fire Mater.* **2023**, *47*, 774–783.
31. Du, D.; Shen, X.; Feng, L.; Hua, M.; Pan, X. Efficiency Characterization of Fire Extinguishing Compound Superfine Powder Containing $Mg(OH)_2$. *J. Loss Prev. Process Ind.* **2019**, *57*, 73–80. [CrossRef]
32. Huang, D.; Wang, X.; Yang, J. Influence of Particle Size and Heating Rate on Decomposition of BC Dry Chemical Fire Extinguishing Powders. *Part. Sci. Technol.* **2015**, *33*, 488–493. [CrossRef]
33. Wang, Q.; Jiang, X.; Deng, J.; Luo, Z.; Wang, Q.; Shen, Z.; Shu, C.-M.; Peng, B.; Yu, C. Analysis of the Effectiveness of $Mg(OH)_2/NH_4H_2PO_4$ Composite Dry Powder in Suppressing Methane Explosion. *Powder Technol.* **2023**, *417*, 118255. [CrossRef]


**Disclaimer/Publisher's Note:** The statements, opinions and data contained in all publications are solely those of the individual author(s) and contributor(s) and not of MDPI and/or the editor(s). MDPI and/or the editor(s) disclaim responsibility for any injury to people or property resulting from any ideas, methods, instructions or products referred to in the content.